

# Near-infrared spectroscopic applications for diagnosis of endometrial carcinoma

**Yuhong Xiang**

**Ke Xu**

**Zhuoyong Zhang**

Capital Normal University  
Department of Chemistry  
Beijing, China 100048

**Yinmei Dai**

Capital University of Medical Science  
Beijing Obstetrics and Gynecology Hospital  
Beijing, China 100006

**Peter de B. Harrington**

Ohio University  
Department of Chemistry and Biochemistry  
Center for Intelligent Chemical Instrumentation  
Athens, Ohio 45701-2979

**Abstract.** NIR spectra of 77 endometrium sections (malignant, hyperplasia, and normal samples) are collected. Partial least squares discriminant analysis (PLS-DA) and fuzzy rule-building expert systems (FuRES) are used for classification based on the NIR spectral data. The classification ability of two classifiers is evaluated by using ten bootstraps and five Latin partitions. The results indicate that the classification ability of FuRES is better than that of PLS-DA. The sensitivity, specificity, and accuracy obtained from FuRES for malignant endometrium diagnosis are  $90.0 \pm 0.7$ ,  $95.0 \pm 0.8$ , and  $93.1 \pm 0.8\%$ , respectively. The results demonstrate that NIR spectroscopy combined with the FuRES technique is promising for the classification of endometrial specimens and for practical diagnostic applications. © 2010 Society of Photo-Optical Instrumentation Engineers. [DOI: 10.1117/1.3512183]

**Keywords:** endometrial carcinoma; near-infrared spectroscopy; fuzzy rule-building expert system; bootstrapped Latin partitions.

Paper 10313R received Jun. 6, 2010; revised manuscript received Sep. 13, 2010; accepted for publication Sep. 23, 2010; published online Nov. 19, 2010.

## 1 Introduction

Endometrial carcinoma is the third major cause of gynecologic cancer death (behind ovarian and cervical cancer). Currently, it is the most common malignancy of the female genital tract in industrialized countries and is increasingly prevalent throughout the world year by year.<sup>1</sup>

Traditional diagnostic tests for endometrial carcinoma involve fractional curettage, which has some disadvantages and limitations, including: 1. blind curettage can cause the identification of small lesions to be missed; 2. biased evaluations of tumor location, grade, and penetration depth in the myometrium can lead to high false-positive rates;<sup>2</sup> and 3. it is sometimes difficult to distinguish differentiated tissues between endometrial carcinoma and highly atypical hyperplasia in pathology. Consequently, there is an urgent demand for developing an accurate, rapid, and inexpensive approach to diagnose endometrial carcinoma.

Near-infrared spectroscopy (NIRS) has been successfully applied in noninvasive pathology studies. The absorption of near-infrared radiation ( $14,700$  to  $4000$   $\text{cm}^{-1}$ ) provides qualitative and quantitative information about the chemical composition of physical tissues. Any alteration in the composition of the tissues can be detected and used for diagnostic purposes. Most of the NIRS investigations dealing with human tissues were on breast.<sup>3,4</sup> Other NIRS studies including cervix,<sup>5</sup> brain,<sup>6</sup> skin,<sup>7</sup> prostate,<sup>8</sup> lung,<sup>9</sup> head and neck,<sup>10</sup> pancreas,<sup>11</sup> and colorectal tissues have also been reported.<sup>11</sup> The goals of these studies were to disclose absorption peaks of one or more chromophores, characterizing the differences between malignant and normal tissues.

Chemometrics provides a powerful tool for researchers to extract qualitative and quantitative information effectively from

overlapped NIR peaks. Many pattern recognition techniques are widely used for classification such as partial least squares discriminant analysis (PLS-DA),<sup>12</sup> cluster analysis (CA),<sup>13</sup> artificial neural network (ANN),<sup>14</sup> SIMCA,<sup>15</sup> etc.

The aim of our work is to develop a new chemometric method to diagnose endometrial carcinoma based on the NIR spectra of endometrial tissues. The NIR spectra of endometrial specimens were collected and preprocessed. PLS-DA and fuzzy rule-building expert system (FuRES) models were used for discriminating various classes of samples. The better results of the FuRES classifier were obtained with sensitivity of  $90.0 \pm 0.7\%$ , specificity of  $95.0 \pm 0.8\%$ , and prediction accuracy was  $93.1 \pm 0.8\%$  for detecting patients with endometrial carcinoma.

## 2 Theory

FuRES is a multivariate classifier based on information theory for modeling data in the form of an easy-to-interpret classification tree.<sup>16</sup> Using the iterative dichotomiser 3 (ID3) algorithm, FuRES provides local modeling and implements conjugate gradient optimization for the global minima of fuzzy classification entropy. By this algorithm, a decision tree was constructed, taking the whole set of samples as a root node. Then it partitions the samples at each branch until all the samples belong to one class at each leaf (i.e., terminal node). A classification tree is constructed with fuzzy logic applied at each. Fuzzy classifiers are robust, so that outlying data objects would not cause the model to degrade as in other least squares classifiers.<sup>16</sup>

PLS is a multivariate statistical technique for modeling a relationship between dependent variables ( $Y$ ) and independent variables ( $X$ ). PLS-DA aims to find the variables and directions in multivariate space that discriminate the known classes in the

Address all correspondence to: Zhuoyong Zhang, Capital Normal University, Department of Chemistry, Beijing, China 100048. Tel: 86-010-689-3047. E-mail: gusto2008@vip.sina.com.

calibration set. In our work, a set of binary codes, [1 0 0], [0 1 0], and [0 0 1], were used to represent three types of pathological sections of endometrium tissue.

The bootstrapped Latin partitions (BLPs) method can provide an unbiased evaluation of pattern recognition models.<sup>17</sup> The method was developed based on traditional cross-validation and resampling methods. With the Latin-partition method, block cross-validation is implemented. The dataset is randomly partitioned into  $n_{part}$  equally sized blocks. One group is left out for validation and the others are used for model building. Each group is used once for prediction and ( $n_{part} - 1$ ) times for training. The objects are each used once and only once for prediction, so that the results for the dataset can be pooled. Bootstrapping is a resampling method that uses sampling with replacement.<sup>18</sup>

The prediction error is averaged among the bootstraps, and the standard deviation of the errors allows confidence intervals to be calculated. Therefore, the use of bootstrapped Latin-partition validation can help characterize the inherent variations in the data that result from different partitions between the training and prediction datasets.<sup>19</sup>

### 3 Materials and Method

A Nicolet 6700 (Thermo Scientific, Waltham, Massachusetts) extended Fourier transform near-infrared (FT-NIR) spectrometer (Thermo Electron) equipped with an InGaAs detector was used for the NIR measurement. The spectrometer was controlled by OMNIC service software, version 7.3. Data analysis was done using MATLAB software (The MathWorks Incorporated, South Natick, Massachusetts).

A total of 77 pathological sections of endometrium tissue were provided by Beijing Obstetrics and Gynecology Hospital affiliated with Capital Medical University, Beijing. The histopathological diagnoses indicated that the 77 cases were divided into three groups, including 29 cases of endometrial carcinoma with the age of patients between 35 and 71, 30 cases of endometrial hyperplasia within ages 29 to 63, and 18 cases of normal endometrium tissue within ages 19 to 35. Tissue specimens were prepared as routine paraffin sections.

The NIR spectra of pathological sections were collected by an optical integrating sphere system at room temperature with diffuse reflectance mode. All sections were scanned from  $4000\text{ cm}^{-1}$  to  $10,000\text{ cm}^{-1}$ , and the spectrum of each sample was obtained as a mean of 64 scans, with a resolution of  $4\text{ cm}^{-1}$ . Each section was measured at five different locations, and the average spectra of tissue sections were used as the spectra of cases in the following analysis.

### 4 Results and Discussions

The spectra were first smoothed using the Savitzky-Golay algorithm with a five-point cubic polynomial to eliminate high-frequency noise and baseline drift, followed by multiplicative scatter correction (MSC) to correct the baseline effects caused by physical conditions, such as optical path length, thickness, and medium of sections. The spectra were normalized to unit length and the average of all the normalized spectra was subtracted from each spectrum.

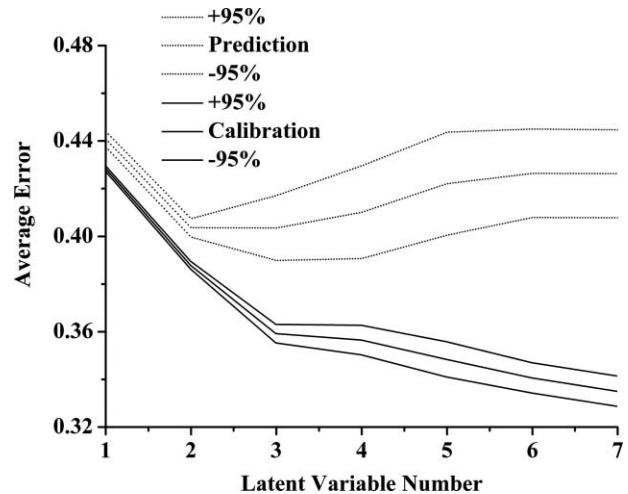


Fig. 1 Effect of the latent variable numbers on averages of calibration error (solid line) and prediction errors (dashed line).

Principal component analysis (PCA) was applied to visualize differences among the samples. The principal component scores show that the three classes of samples are not resolved.

The average values of calibration and prediction errors with respect to latent variable number are given in Fig. 1, with 95% confidence intervals obtained from ten bootstraps and five Latin partitions. The latent variable number of 3 was chosen based on this evaluation.

A confusion matrix obtained from the average prediction results of ten bootstraps is given in Table 1. In this matrix, the rows represent the true class, and columns represent the predicted class. The average values of the ten bootstraps are presented with 95% confidence intervals. In this test, the sensitivity was  $77.9 \pm 2.1\%$ , the specificity was  $65.6 \pm 2.1\%$ , and prediction accuracy was  $70.3 \pm 2.1\%$  for detecting malignant samples.

FuRES constructs a classification tree that allows the visualization of the inductive structure of the rules. Membership functions in FuRES allow values between 0 and 1 and provide a measure of the degree of similarity of elements in the total population.<sup>20</sup>

Table 1 The confusion matrices obtained from the validations of PLS-DA and FuRES classifiers.

|                     | Malignant      | Hyperplasia    | Normal         |
|---------------------|----------------|----------------|----------------|
| <b>PLS-DA model</b> |                |                |                |
| Malignant           | $22.6 \pm 0.6$ | $5.4 \pm 0.6$  | $1.0 \pm 0$    |
| Hyperplasia         | $15.3 \pm 0.9$ | $13.5 \pm 1.0$ | $1.2 \pm 0.2$  |
| Normal              | $0 \pm 0$      | $0 \pm 0$      | $18.0 \pm 0$   |
| <b>FuRES model</b>  |                |                |                |
| Malignant           | $26.1 \pm 0.2$ | $1.9 \pm 0.2$  | $1.0 \pm 0$    |
| Hyperplasia         | $0.5 \pm 0.3$  | $28.0 \pm 0.5$ | $1.5 \pm 0.5$  |
| Normal              | $0.4 \pm 0.3$  | $0 \pm 0$      | $17.6 \pm 0.3$ |

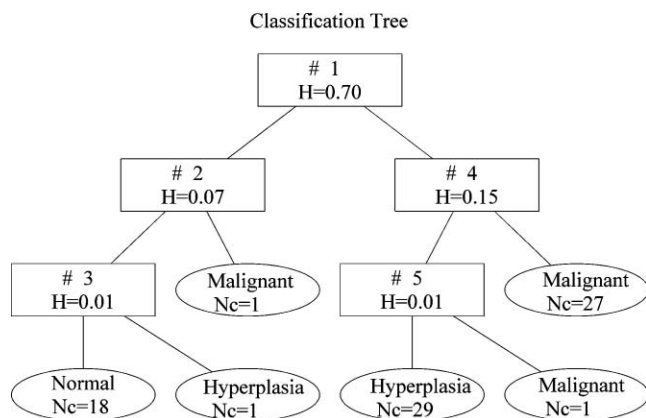


**Fig. 2** The FuRES classification tree of the entire dataset after preprocessing. The numbers (Nc) and names of samples were labeled in each leaf node. The values of fuzzy entropy (H) corresponding to rules 1 through 5 are given in the rectangles.

A FuRES classification tree built from the entire dataset consisting of 77 samples is given in Fig. 2. The logistic value of fuzzy entropy generated by the first rule was 0.70, and samples were separated for two subsets. The classification entropy of the system decreases as the classification tree branches.

As in the PLS-DA evaluation, the FuRES models were evaluated by using ten bootstraps and five Latin partitions. The prediction results were pooled among the five Latin partitions, and the average predictions of the ten bootstraps are reported with 95% confidence intervals.

The prediction results for FuRES are also given in Table 1. The sensitivity for detecting malignant samples was  $90.0 \pm 0.7\%$ , the specificity was  $95.0 \pm 0.8\%$ , and prediction accuracy was  $93.1 \pm 0.8\%$ , which were better than those by PLS-DA. A plausible explanation for the difference in performance is that the FuRES model is accommodating three outlier points in rules 3, 4, and 5. The fuzziness of the model prevents these outliers from having a detrimental effect on the classification model. These outlier samples could be driving the PLS-DA model into an ill-conditioned solution, as would be expected for any least squares classifier. The effect of outlier spectra during BLP results in wide precision bounds in Fig. 1 and wider intervals in the prediction results for nonrobust classifiers. The results suggest that the FuRES classifier performed a soft pattern recognition that exhibits robustness and better prediction accuracy than PLS-DA for detection of endometrial cancerous tissues by NIRS.

## 5 Conclusion

Based on the NIR spectra of 77 pathological endometrial sections, classification models are constructed to diagnose endometrial cancer by using PLS-DA and FuRES. Classification accuracy from the PLS-DA model is insufficient. The FuRES classifier significantly improves the accuracy of classification. This classifier is evaluated using ten bootstraps and five Latin partitions that yield an average prediction accuracy of  $93.1 \pm 0.8\%$ , a sensitivity of  $90.0 \pm 0.7\%$ , and a specificity of  $95.0 \pm 0.8\%$  for detecting malignant samples. The results suggest that near-infrared spectroscopy combined with FuRES

provide a powerful tool for the detection of early endometrial carcinoma. This method could be developed into a noninvasive method for clinical diagnosis for other cancers.

## Acknowledgments

This work was supported by the National Natural Science Foundation of China (grant numbers 20875065 and 30772322), Beijing Municipal Natural Science Foundation (2102010), and Funding Project for Academic Human Resources Development in Institutions of Higher Learning Under the Jurisdiction of Beijing Municipality (PHR20100718).

## References

1. A. Doll, M. Gonzalez, M. Abal, M. Llauro, M. Rigau, E. Colas, M. Monge, J. Xercavins, G. Capella, B. Diaz, A. Gil-Moreno, F. Alameda, and J. Reventos, "An orthotopic endometrial cancer mouse model demonstrates a role for RUNX1 in distant metastasis," *Int. J. Cancer* **125**(2), 257–263 (2009).
2. M. Q. Bernardini and J. K. Murphy, "Issues surrounding lymphadenectomy in the management of endometrial cancer," *J. Surg. Oncol.* **99**(4), 232–241 (2009).
3. B. J. Tromberg, A. Cerussi, N. Shah, M. Compton, A. Durkin, D. Hsiang, J. Butler, and R. Mehta, "Diffuse optics in breast cancer: detection tumors in pre-menopausal women and monitoring neoadjuvant chemotherapy," *Breast Cancer Res.* **7**(6), 279–285 (2005).
4. A. Cerussi, N. Shah, D. Hsiang, A. Durkin, J. Butler, and B. J. Tromberg, "In vivo absorption, scattering, and physical properties of 58 malignant breast tumors determined by broadband diffuse optical spectroscopy," *J. Biomed. Opt.* **11**(4), 044005 (2006).
5. Y. N. Mirabal, S. K. Chang, E. N. Atkinson, A. Malpica, M. Follen, and R. Richards-Kortum, "Reflectance spectroscopy for in vivo detection of cervical precancer," *J. Biomed. Opt.* **7**(4), 587–594 (2002).
6. S. Asgari, H. J. Röhrborn, T. Engelhorn, and D. Stolke, "Intra-operative characterization of gliomas by near-infrared spectroscopy: possible association with prognosis," *Acta Neurochir.* **145**(6), 453–460 (2003).
7. E. Salomatina, B. Jiang, J. Novak, and A. N. Yaroslavsky, "Optical properties of normal and cancerous human skin in the visible and near-infrared spectral range," *J. Biomed. Opt.* **11**(6), 064026 (2006).
8. J. H. Ali, W. B. Wang, M. Zevallos, and R. R. Alfano, "Near infrared spectroscopy and imaging to probe differences in water content in normal and cancer human prostate tissues," *Technol. Cancer Res. Treat.* **3**(5), 491–497 (2004).
9. M. P. L. Bard, A. Amelink, V. N. Hegt, W. J. Graveland, H. J. C. M. Sterenborg, H. C. Hoogsteden, and J. G. J. V. Aerts, "Measurement of hypoxia-related parameters in bronchial mucosa by use of optical spectroscopy," *Am. J. Respir. Crit. Care Med.* **171**(10), 1178–1184 (2005).
10. U. Sunar, H. Quon, T. Durduran, J. Zhang, J. Du, C. Zhou, G. Yu, R. Choe, A. Kilger, R. Lustig, L. Loevner, S. Nioka, B. Chance, and A. G. Yodanis, "Noninvasive diffuse optical measurement of blood flow and blood oxygenation for monitoring radiation therapy in patients with head and neck tumors: a pilot study," *J. Biomed. Opt.* **11**(6), 064021 (2006).
11. V. R. Kondepati, T. Oszinda, H. M. Heise, K. Luig, R. Mueller, O. Schroeder, M. Keese, and J. Backhaus, "CH-overtone regions as diagnostic markers for near-infrared spectroscopic diagnosis of primary cancers in human pancreas and colorectal tissue," *Anal. Bioanal. Chem.* **387**(5), 1633–1641 (2007).
12. R. M. Balabin, R. Z. Safieva, and E. I. Lomakina, "Comparison of linear and nonlinear calibration models based on near infrared (NIR) spectroscopy data for gasoline properties prediction," *Chemo. Intell. Lab. Sys.* **88**(2), 183–188 (2007).
13. V. R. Kondepati, M. Keese, R. Mueller, B. C. Manegold, and J. Backhaus, "Application of near-infrared spectroscopy for the diagnosis of colorectal cancer in resected human tissue specimens," *Vibr. Spectrosc.* **44**(2), 236–242 (2007).

14. X. L. Li and Y. He, "Discriminating varieties of tea plant based on Vis/NIR spectral characteristics and using artificial neural networks," *Biosyst. Eng.* **99**(3), 313–321 (2008).
15. O. Y. Rodionova, L. P. Houmøller, A. L. Pomerantsev, P. Geladi, J. Burger, V. L. Dorofeyev, and A. P. Arzamastsev, "NIR spectrometry for counterfeit drug detection: a feasibility study," *Anal. Chim. Acta* **549**(1–2), 151–158 (2005).
16. P. B. Harrington, N. E. Vieira, P. Chen, J. Espinoza, J. K. Nien R. Romero, and A. L. Yergey, "Proteomic analysis of amniotic fluids using analysis of variance-principal component analysis and fuzzy rule-building expert systems applied to matrix-assisted laser desorption/ionization mass spectrometry," *Chem. Intel. Lab. Syst.* **82**(1–2), 283–293 (2006).
17. C. H. Wan and P. D. Harrington, "Screening GC-MS data for carbamate pesticides with temperature-constrained-cascade correlation neural networks," *Anal. Chim. Acta* **408**(1-2), 1–12 (2000).
18. G. L. Grunkemeier and Y. X. Wu, "Bootstrap resampling methods: something for nothing," *Ann. Thor. Surg.* **77**(4), 1142–1144 (2004).
19. P. B. Harrington, "Statistical validation of classification and calibration models using bootstrapped Latin partitions," *Tr. Anal. Chem.* **25**(11), 1112–1124 (2006).
20. P. Rearden, P. B. Harrington, J. J. Karnes, and C. E. Bunker, "Fuzzy rule-building expert system classification of fuel using solid-phase microextraction two-way gas chromatography differential mobility spectrometric data," *Anal. Chem.* **79**(4), 1485–1491 (2007).